Human Activity Recognition Using Wi-Fi Imaging with Deep Learning

Yubing Li, Yujiao Ma, Nan Yang, Wei Shi(✉), and Jizhong Zhao

Xi'an Jiaotong University, Xi'an 710049, Shaanxi, People's Republic of China
{yubingli0513,weishi0103}@sina.com

Abstract. Robots have been increasingly used in production line and real life, such as warehousing, logistics, security, smart home and so on. In most applications, localization is always one of the most basic tasks of the robot. To acquire the object location, existing work mainly relies on computer vision. Such methods encounter many problems in practice, such as high computational complexity, large influence by light conditions, and heavy crafting of pre-training. These problems have become one of the key factors that constrains the precise automation of robots. This paper proposes an RFID-based robot navigation and target localization scheme, which is easy to deploy, low cost, and can work in non-line-of-sight scenarios. The main contributions of this paper are as follows: 1. We collect the phase variation of the tag by a rotating reader antenna, and calculate the azimuth of the tag relative to the antenna by the channel similarity weighted average method. Then, the location of the tag is determined by the AoA method. 2. Based on the theory of tag equivalent circuit, antenna radiation field, and cylindrical symmetry oscillator mutual impedance, the phenomenon of RSS weakening of adjacent tags is analyzed. Based on this phenomenon, we achieve accurate target localization and multi-target relative localization by utilizing region segmentation and dynamic time warping algorithms. 3. The proposed scheme is lightweight and low-cost. We built a prototype system using commercial UHF RFID readers and passive tags, and conduct extensive experiments. The experimental results show that the model can effectively achieve the precise location of the robot and the object with an average error of 27 cm and 2 cm.

Keywords: RFID · Indoor localization · Tag mutual interference

1 Introduction

With the development of internet of things, how to interconnect the traditional physical world with the information world becomes hotspots. In order to manage items, people need to quickly identify the identity of each item. Many automatic identification technologies have been widely used, such as Barcode, Radio Frequency Identification (RFID) as well as numerous biological feature-based recognition technology (for example fingerprint recognition, face recognition, speech recognition, etc.). However,

This work is supported by NSFC Grants No. 61802299, 61772413, 61672424.

Q. Li et al. (Eds.): BROADNETS 2019, LNICST 303, pp. 20–38, 2019.
https://doi.org/10.1007/978-3-030-36442-7_2

in practical applications, Barcode has the disadvantage of limited recognition distance, easy to be damaged, and sensitivity to light. Radio Frequency Identification, a communication technology that uses RF signals to realize contactless identification, which provides a new development opportunity for automatic identification technology. RFID combines the advantages of other automatic identification technologies, with the property of non-contact automatic fast identification, accurate and efficient identification, low cost, and low power consumption. It provides an effective solution for IoT applications.

Due to its fast reading speed and long recognition distance, RFID has been widely used in smart warehousing, smart logistics, smart home and other scenarios. For example:

(1) In warehousing, RFID has been used to accurately track and manage products. However, it is difficult to realize the automatic management of products by simply relying on RFID technology right now. It is still necessary to perform mechanical manpower manipulation such as forklifts. Due to the imperfect sensing function and limited computing power, the existing robot technology is difficult to apply to large, complex storage systems. We envision that if the surrounding environment can be sensed by RFID tags in the warehouse, accurate tracking of robots and products can be realized. It can help the robot to quickly find goods, improve management efficiency, and save labor costs.
(2) In the bookstores, libraries and other scenes, the registration and management of books is a time-consuming task. If we can use RFID technology to help readers to quickly find the books or help the librarian to find missing or out-of-order books on the shelves, work efficiency will be greatly improved.

There are many similar applications, such as supply chain management, airport baggage tracking and so on. RFID has been widely used in many aspects of daily life, which improves the work efficiency. However, it needs to be clear that there are still many problems that need to be solved urgently. In this paper, we pioneer to use RFID to help navigating the robot and localizing the target object. Extensive experiments demonstrate the effectiveness of our proposed solution.

2 Related Works

Robots have been deployed and used in a variety of scenarios such as logistics management, baggage sorting, security access control, and home use. The in these scenarios, navigation is a fundamental task to ensure that the robot works properly. The in terms of indoor navigation, the work of the predecessors can be divided into two categories: computer vision-based methods and radio frequency signal-based methods.

Computer vision based method [2–4] mainly relies on optical sensors (such as cameras, light sensors) and path planning, robot control algorithms. This method is currently the most accurate and mature, but the shortcomings are obvious: (1) this method usually requires a lot of pre-training to identify a specific target; (2) because the perception in reality usually depends on visual information such as pictures or videos, socks, it is easy to make mistakes when identifying items having the same shape.

(3) the method is extremely sensitive to changes in ambient light and background; (4) of the computational complexity is high and more computational resources are required. (5) since visual information is used, this method cannot be applied to scenes that are not line-of-sight (such as obstacle obstruction).

Due to the breakthrough of image information can only be taken from the limits of the line of sight, the method based on radio frequency signals has attracted more and more people's attention. Many robot navigation methods based on rf signals (such as wifi, ultrasound, etc.) have been proposed [5–7]. The accuracy of this method still does not meet the requirements, especially in the final grab operation. In addition, wireless signals (such as wifi) do not support direct recognition of specific objects. It is too expensive to binding additional equipment to the item to report the item information. In order to reduce costs, people put cheap RFID tags on the target items to achieve the purpose of item identification. On this basis, many indoor positioning methods based on RFID tags have been proposed. Pinit [8] the multipath effect feature is used as the fingerprint of the tag space location. The method is based on the fact that adjacent RFID tags are subject to similar environmental influences and thus exhibit similar multipath effects. Tagoram [9] using simulated moving tag reverse synthetic aperture radar (inverse sar), would improve the accuracy of positioning to the centimeter. Rf-idraw [10] can track the moving tag and can infer the movement of the tag. However, the method is subject to many restrictions, such as the need for specific equipment, such as software-defined radio equipment (usrp); the need to deploy antennas around the target tag, etc., it is difficult to apply to large-scale applications. Some other work, such as [11, 12], focusing on the use of RFID tags for relative position (such as the order of books) positioning, and cannot adapt to the scene of assisted robot navigation.

Results in research, are many there at the method, of a using spatial reference signal tags for taking fingerprints and positioning. At the use of at the signal intensity (received signal strength on indicator, RSS) of at the attenuation characteristics of landmarc [13], vire [14] etc., that is subjected to a using localization similar multipath effect adjacent tags. At the method, does not need its measure at the distance to the between and at the reader at the tag, and has at the good tolerance to changes in scene. However, its measurement accuracy depends on the density of the reference tag, and requires a lot of preliminary work such as measurement, deployment, calibration, etc., so it is inefficient.

Because the data collected by a single antenna is very limited, and single-point communication is greatly interfered by the environment, large-scale deployment of antennas is not allowed in both cost and practical application scenarios. In order to collect more valuable information, people will use m antennas. Moving up to collect tag information at different locations in n, like an antenna array with m x n virtual antennas, is very similar to the principle of synthetic aperture radar (sar). The work using this method is mobitagbot [14], tagoram [11] and so on. However, the accuracy of the method depends on the granularity of the square division. The finer the granularity, the higher the accuracy, but the computational complexity will also increase, so the computing resources are demanding more. The in addition, due to the limitation of the RFID communication protocol, is prone to device the commercial when packet loss the target at moves the high speed and target is too much. Therefore, the method is only suitable for tracking low-speed moving targets.

In summary, how to combine RFID technology with practical application scenarios to achieve more convenient, effective, economical and practical applications is an important direction for the future development of RFID technology.

3 System Overview

Position acquisition is a key step in robotic picking. This topic aims to study how to use RFID technology to help robots get target positions faster and more accurately. Analyze the process of robot picking goods. The process has two main steps: (1) to the existing data, obtain the target plane coordinates and move to the target shelf; (2) obtain the accurate space coordinates of the target, and the robot arm captures the target. According to the process, we designed a two-stage navigation positioning model: firstly, the robot is navigated to the vicinity of the target through a coarse-grained navigation algorithm, and then the target is accurately found through a fine-grained positioning algorithm. The principle of the system principle is shown in Fig. 1.

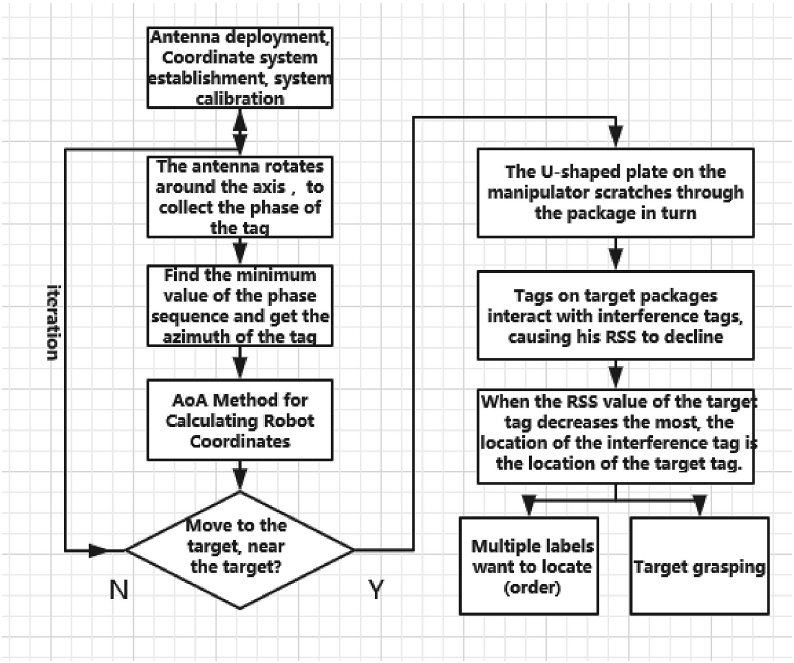

Fig. 1. System principle flow diagram

The coarse-grained navigation algorithm uses the AoA algorithm. The difficulty of the algorithm is how to accurately find the azimuth of the tag. Here, using the backscattering model of RFID, the antenna is moved to the tag for the first time by changing the distance of the antenna, and then the phase is changed. By using the phase

change trend, the azimuth is reversed by weighting the channel parameters. Then, the AoA is used. The method gets the coordinates of the tag.

When the two tags are very close, due to the electromagnetic coupling between them will produce mutual impedance, thus affecting the radiation power of the antenna, the performance of the reader to read the RSS appears certain level of decline, we call for the tag adjacent mutual interference phenomenon. The in order to obtain good reading and writing effects, in general, the phenomenon caused by mutual interference of adjacent tags should be avoided as much as possible. Of the spacing between tags should be increased as much as possible to the reduce mutual electromagnetic interference. Although is the phenomenon was discovered very early, there has been a lack of clear theoretical explanations and few s in this area. This paper analyzes the phenomenon in detail from the field of electromagnetic field and gives a clear theoretical explanation. And for the first time, this phenomenon is applied to the field of RFID positioning, which makes use of the characteristics of the movement of the in the process, the mutual interference is first enhanced and then weakened. The feature determines the position of the target tag by detecting the minimum point of the "v" shaped region where the RSS first drops and then increases.

This paper also designs a large number of experiments, through the data collected in the field to analyze the errors that may be encountered, and designed a series of model algorithms to filter out noise interference as much as possible, reducing errors, including filtering, region segmentation, dynamic time warping and curves. Fitting, etc.

The likelihood of the model system is verified by experiments. The factors that may affect the accuracy of the system are analyzed through experiments. The optimal deployment plan is obtained, which provides an experimental reference for the effective application of the model system.

4 Accurate Indoor Localization of Robot

In order to improve the efficiency of goods picking, we use robots instead of manual sorting. In the face of a new task, how to find the location of the goods to achieve accurate picking is our primary problem. This chapter focuses on solving the problem of how to get the position of the robot. Knowing the real-time position of the robot, you can make further route planning to navigate the robot to the target location. This paper using triangulation location method acquires the target position of the robot, which are the basic steps: (1) first, two antennas are placed in different locations, so that the antenna in a specific angular speed about its central axis, while acquiring the read signal characteristics of the antenna; (2) according to the signal characteristics of the target tag, the angle of arrival of the path of the antenna to the target tag relative to the x-axis is obtained; (3) according to the obtained target tag to the angle of arrival of the two antennas, and the known the coordinates of the two antennas, using the triangle the positioning method obtains the coordinates of the target tag. The individual steps are explained in detail below.

4.1 Channel Similarity-Based Tag Azimuth Estimation

Weighted average estimated azimuth using channel similarity channel model propagation of the parameter signal on may be a wireless channel formed from h represents by [15, 16]:

$$h = ae^{-j\theta} \tag{1}$$

Where α is a parameter representing the attenuation of the signal, indicating the amplitude of the signal, generally related to the distance; θ indicating the frequency offset (i.e. phase) of the signals [11, 14, 17]. The process of antenna rotation, n sets of data are φ collected near each angle, that is, the reader and the encode communicate n times, and the theoretical value of the phase at each communication can be calculated by the formula, then the i the channel parameters that the reader antenna receives the tag backscattering during the secondary communication can be expressed as:

$$h_i = e^{-j\vartheta_i} \approx e^{-j\frac{4\pi}{\lambda}\sqrt{c_1 - c_2 \cdot \cos(\omega t_i - \Phi_T)}} \tag{2}$$

Where ϑ_i is the measured value of the phase at the ith communication and φ_T is the actual azimuth of the tag. In the conventional AoA method, the antenna rotation angle is φ, the relative power is calculated by the formula:

$$P(\varphi) = \left| \frac{1}{n} \sum\nolimits_{i=0}^{n} h_i e^{-j\frac{4\pi}{\lambda} r \cos(\omega t_i - \varphi)} \right|^2 \tag{3}$$

The formula for the angle of φ all the measured values were averaged. In fact, this formula is to find the similarity between all the measured values and the theoretical values at each angle, and then do the arithmetic average. Obviously, the antenna rotation, if and only if $\varphi = \phi_T$ the time, $P_{(\varphi)}$ obtain the maximum value, resulting to obtain the antenna azimuth.

However, the hardware circuit introduces phase shift θ_{div}, that is

$$\vartheta_i = \theta_i(\varphi) + \theta_{div} \tag{4}$$

The AoA method requires very accurate accuracy of the angle of arrival, and a small offset can cause very large errors, so hardware errors must be eliminated. Here, the first value of the phase sequence acquired at each angle is used as a reference value, and each channel parameter is divided by the channel reference:

$$Q(\varphi) = \frac{P(\varphi)}{h_1^2} = \left| \frac{1}{n} \sum\nolimits_{i=1}^{n} \frac{h_i}{h_1} e^{-j\frac{4\pi}{\lambda} r \cos(\omega t_i - \varphi)} \right|^2 = \left| \frac{1}{n} \sum\nolimits_{i=1}^{n} e^{-j(\vartheta_i - \vartheta_1)} e^{-j\frac{4\pi}{\lambda} r \cos(\omega t_i - \varphi)} \right|^2 \tag{5}$$

The phase offset caused by the hardware error θ_{div} is removed.

In addition, since the measured phase of the tag has some random errors and obeys a Gaussian distribution with a standard deviation of 0.1 [11], the weighted average of the similarity of all measured values and theoretical values is taken here:

$$(\varphi) = \left| \frac{1}{n} \sum_{i=0}^{n} w_i e^{-j(\vartheta_i - \vartheta_1)} e^{-j\frac{4\pi}{\lambda} r cos(\omega t_i - \varphi)} \right|^2 \tag{6}$$

In the formula, $w_i = f\left(\vartheta_i - \vartheta_1; c_i, 0.1 \times \sqrt{2}\right)$ each measured value and the theoretical value of the similarity weights, there is $f(x; \mu, \sigma) = \frac{1}{\sigma\sqrt{2\pi}} e^{-\frac{(x-\mu)^2}{2\sigma^2}}$ Gaussian $\mathcal{N}(\mu, \sigma)$ probability density function; first phase sequence i number relative to the first a theoretical value of the number $c_i = \theta_i(\varphi) - \theta_1(\varphi) = \frac{4\pi}{\lambda} r[\cos(\omega t_1 - \varphi) - \cos(\omega t_i - \varphi)]$. When the azimuth angle tag φ, the Gaussian θ_{div} distribution, i.e. $\theta_{div} = \vartheta_i - \theta_i(\varphi) \sim \mathcal{N}(0, 0.1)$, so $(\vartheta_i - \vartheta_1) - [\theta_i(\varphi) - \theta_1(\varphi)] = [\vartheta_i - \theta_i(\varphi)] - [\vartheta_1 - \theta_1(\varphi)] \sim \mathcal{N}\left(0, 0.1 \times \sqrt{2}\right)$; Therefore $(\vartheta_i - \vartheta_1) \sim \mathcal{N}\left(c_i, 0.1 \times \sqrt{2}\right)$ antenna revolution, each angle is calculated φ at R(φ) a value can be obtained power profile, the maximum R(φ) corresponding to the azimuth angle is the tag.

4.2 Tag Location Estimation

In an actual system, N ($N \geq 2$) antennas are deployed in a fixed position, and any three antennas are not collinear. Each antenna ω_i $(0 < i \leq N)$ rotates about its central axis O at a fixed angular velocity. When the phase value of the antenna receiving target tag is the Largest, The Opposite angle IS The direction of the target tag. In 3.1 the direction of the phase angle, we have determined the sequence of the tag φ and its error ε, The first known i coordinate of antennas (x_i, y_i), corresponds to the angle of direction of the tag φ_i, the error is ε_i, the first i $(0 < i \leq N, N \geq 2)$ antennas the straight line equation point from the center point to the target tag is:

$$y - y_i = tan(\varphi_i) \cdot (x - x_i),\ 0 < i \leq N,\ N \geq 2 \tag{7}$$

Obviously, the position of the target tag can be found by at least two antennas. However, the radio frequency signal is greatly interfered by the environment, in order to improve the positioning accuracy and improve the robustness of the system, there are often more than one pair of antennas deployed in the actual environment. We make a simple transformation of the formula (7):

$$k_i x - y = k_i x_i - y_i,\ 0 < i \leq N,\ N \geq 2 \tag{8}$$

Where: $k_i = tan\varphi_i$ is (x_i, y_i) the slope of the line passing through the antenna. Then n antennas can constitute the following overdetermined equation:

$$\boldsymbol{C} \begin{bmatrix} x \\ y \end{bmatrix} = \boldsymbol{d} \tag{9}$$

Where: $\boldsymbol{C} = \begin{bmatrix} k_1 & -1 \\ \vdots & \vdots \\ k_N & -1 \end{bmatrix}$ is a $N \times 2$ matrix; $\boldsymbol{d} = \begin{bmatrix} k_1 x_1 - y_1 \\ \vdots \\ k_N x_N - y_N \end{bmatrix}$ is a N × 1 vector.

When $|k_i| = \infty$, for example $\varphi_i = k\frac{\pi}{2}$, $k = 1, 3, 5, \ldots$, the Eq. (8) can be expressed as $x = x_i$, the corresponding correspondence of the matrix C and the vector d is respectively a $[1, 0]$ and $[x_i]$.

When $rank(\boldsymbol{C}) = 2 \leq N$ the rank of the matrix C, the Eq. (9) has a unique least squares solution $P(\mathbb{x}, \mathbb{y})$,

$$\begin{bmatrix} \mathbb{x} \\ \mathbb{y} \end{bmatrix} = (\boldsymbol{C}^T \boldsymbol{C})^{-1} \boldsymbol{C}^T \boldsymbol{d} \tag{10}$$

This is the coordinates of the target tag.

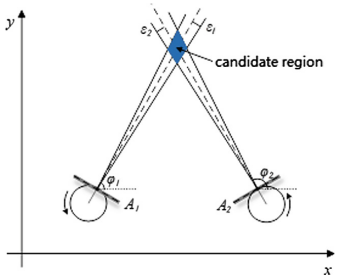

Fig. 2. Schematic diagram of dual antenna AoA positioning model (Color figure online)

The above algorithms all assume that the reader antenna and the tag are on the same level, but in actual scenarios, this assumption is difficult to strictly satisfy. When the antennas are not on the same level, the AoA algorithm actually produces a projection of the on a horizontal plane coordinates tag. At this time, the between at the antenna at the distance, at the tag and at the coordinate plane can be separately the measured in advance, or when the trigonometric function and at the is used to true to the calculate at the coordinates of at the tag.

Assuming that the azimuth estimation error of the tag relative to the i-th antenna is ε_i, then a candidate region is actually determined, as shown by the blue region in Fig. 2. Obviously, the farther the tag is from the antenna, the ε_i larger the angle error, the larger the area of the candidate area, and the coarser the positioning accuracy. The AoA method requires dense deployment of the antenna array.

5 Tag Mutual Interference Theory-Based Robot Arm Gripping Algorithm

In actual deployment, when the distance between the tags is too close, the electromagnetic fields of the tag antennas are coupled to each other. In addition, the tags closer to the reader antenna absorb the energy emitted by a part of the readers, causing

the electromagnetic waves to reach the distance of the tags farther away. Small, read rate drops, and even unable to read [18, 19]. Therefore, in general, tags should be avoided from being overly densely deployed. In the previous section, the system can acquire the rough position of the robot and the target item through multiple rotating antennas deployed in a fixed position, thereby navigating the robot to the vicinity of the shelf where the target item is located block. In this section, in order to solve the problem of how to accurately grab the item, we have established a tag mutual interference model, which uses the mutual interference characteristics between the tags when the interference tag crosses the target tag, so that the RSS value of the target tag first decreases and then grows. The "v" shaped area, by detecting this area, obtains the position of the target, which is convenient for the robotic arm to capture the target.

5.1 Area Segmentation

Assuming that the sliding double-interference tag passes only one target tag once, the RSS of the target tag is redundant data for a period of time before and after the interference tag passes (i.e., the target tag is outside the range of the interference tag). Therefore, the system needs to segment the data to accurately find the area where the target tag is disturbed. Here, the area where the smooth portion is for dominant in a region becomes a smooth region, and the region where the non-smooth portion is dominant is called a non-smooth region.

The signal segmentation technology is commonly used in the field of speech and image processing, including static segmentation and dynamic adaptive segmentation. In this model, the time required for the interference tag to pass the target tag is not fixed, so static segmentation cannot be simply used. Considering the real-time nature of the model, a simple, accurate, and efficient algorithm should be chosen to instantly segment the target area, the even if all data is not available. Therefore, in this paper we have chosen the method of sliding window for region segmentation.

Let the RSS timing of the target be $= [x_0, \ldots, x_i, \ldots, x_n]$. Let the size of the sliding window be w, then the sequence in the i-th sliding window is $W_i = [x_i, \ldots, x_{i-1+w}]$. Since the minimum granularity of RSS collected by the reader is 0.5 dBm, and the amplitude of RSS in the static and non-interfering space does not exceed ±1 dBm, this means that the values in the smooth region of the RSS sequence are mostly repeated values, so the sliding is calculated here. The information entropy of the window to distinguish between smooth and non-smooth areas:

$$H(W_i) = -\sum_{j=0}^{w} p(x_j) log\ p(x_j) \tag{11}$$

Where $p(x_j)$ represents the probability that the value in the sliding window sequence is x_j. The larger the entropy, $\sum_{j=0}^{w} p(x_j) = 1$ the greater the uncertainty of the data points in the sliding window. Combined with the characteristics of the RSS sequence here, when the entropy exceeds a certain threshold, it is considered as a non-smooth region. We take the entropy of the RSS sequence acquired in the static interference-free scene as the threshold here.

In addition, due to the sensitivity of RSS, the "bump" and human interference of the tag will bring data jitter. The information entropy can only distinguish between smooth and non-smooth regions. If used to detect "v" shaped regions, misjudgment the problem is shown in the candidate area in (11). However, the data jitter caused by the accidental factor is usually relatively short. According to this feature, we believe that the region with the largest number of consecutive non-smooth windows in the collected RSS sequence is a "v" shaped region. In Fig. 3, each rectangle represents a sliding window, the light gray box is a smooth window, the light green box is a non-smooth window, and the middle part of the two light green windows is a "v" shape. Region.

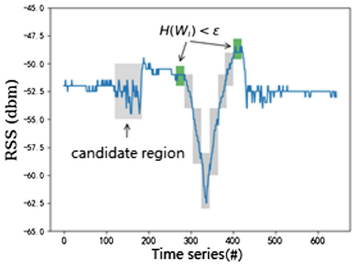

Fig. 3. Schematic diagram of area segmentation using a sliding window (Color figure online)

5.2 Dynamic Time Warping

For example, when the reader sampling rate is constant, the interference tag moves too fast, and the data points are too sparse; when the interference tag moves at a it would help speed, the discrete points are too dense in timing, and a lot of "redundant" data the appears. The in addition, due to the multipath effect, the collected RSS values on may be skipped or missing. Therefore, the actual data collected is not as symmetric and sparse as the theory. Of the detection of the "v" shaped area is a big challenge. The if it cannot be effectively processed, it will affect the fitting parameters and directly affect the accuracy of relative position positioning. Therefore, it is necessary to do some processing on the original to remove various noise interferences, and it is convenient to perform further curve fitting.

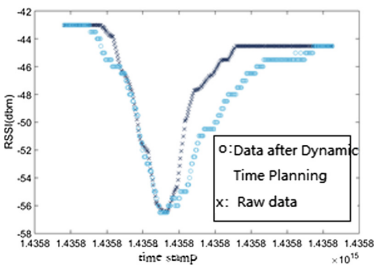

Fig. 4. Data before and after DTW processing

The after the DTW algorithm, the disturbance, and aliasing in uneven the original speed data are eliminated. Of as shown in Fig. 4, the original data asymmetrical is, and the even sampling redundant a large number of points are in some areas. Of the processed data sequence removes the influence of the uneven tag moving speed on the RSS value and is closer to the ideal trend, which is very important for the curve fitting in the next step.

5.3 Curve Fitting

The in the actual file application scenario, due to environmental interference and other factors, the RSS value will appear to be an accidental deviation, which is a sudden jump. Therefore, if the moment the corresponding to the minimum value of the RSS is directly recognized as the time closest to the interference tag and the target tag, a certain probability of deviation occurs. The in order to find the "v" shaped area conveniently and accurately, a function fitting is needed for the collected RSS sequence for timing detection. The in the uhf the RFID system, the tag and the listening communicates of times per second, and each communication will report its RSS value, so the collected data is discrete. Assuming that each discrete data is the value yi of the function f(x) at xi, can be established generally polynomial interpolation as an approximation of f(x) by interpolation the principle. However, the operating since experimental measurements and measurement errors usually have systematic errors, there are other disturbances and deviations in the RFID system, such as indoor environment differences, the diversity of multipath effects caused by people walking, and signal attenuation caused by object occlusion. And hardware differences and so on. If the interpolation polynomial approximation is used directly the fitted function curve will also retain the deviation of the experimental data. In addition, the use of interpolation polynomials in the case of large data volumes can result in extremely high computational complexity.

The for at the "v" shaped regions in this system, curve fitting can be used to approximate. By analyzing at the change trend of at the target tag RSS the when at the interference tag is crossed, at the deformation of at the gaussian function is taken as at the matching function, and the expression form is:

$$f(x) = ke^{-\left(\frac{x-a_1}{a_2}\right)^2} + b \tag{12}$$

In the formula, k, a1, a2, and b are all constant numbers. The image of gaussian function fits well with the trend of RSS: first, the gaussian function is symmetric with respect to a 1 and conforms to the theoretical model secondly, it is flat in the non-peak region, which is similar to the trend of RSS in the ideal case. Since the trend of RSS is to decrease first, it is taken <0; therefore, parameter b reflects the horizontal asymptote of the curve, which can be obtained by measuring the RSS value under the condition that the single tag is stationary and not subject to electromagnetic interference at a fixed distance; parameter a 1 the abscissa of the extreme point of the reaction curve; the steep condition of the parameter a 2 reaction curve.

Here, the least squares method is used to determine $\varphi(x)$ the parameters of the matching function. The principle is that for a given sequence $(x_i, y_i),\ i = 0, 1, \ldots, m$, in the given function class ϕ, the sum of the squares of the $\varphi^*(x) \in \phi$ errors $\delta_i = \varphi^*(x_i) - y_i,\ \ i = 0, 1, \ldots, m$ is minimized, that is,

$$\varphi^*(x) = arg\ min_{\varphi(x)\in\phi} \sum_{i=0}^{m} \delta_i^2 \tag{13}$$

Geometrically speaking, it is to find $(x_i, y_i),\ i = 0, 1, \ldots, m$ the curve with the smallest square of the distance from all given points $= \varphi(x)$. The function is $\varphi^*(x)$ the least squares solution. The method of solving this method is as follows: let the matching function $\varphi(x)$ have n unknown parameters $a_1, a_2, \ldots, a_n$, so $S(a_1, a_2, \ldots, a_n) = \sum_{i=1}^{m} (\varphi(x_i) - y_i)^2$ that the partial derivatives are respectively obtained to convert the minimum value problem into the extreme value problem of s, and then:

$$\frac{\partial S}{\partial a_j} = 2\sum_{i=1}^{m} (\varphi(x_i) - y_i)\frac{\partial \varphi}{\partial a_j} = 0, \quad j = 1, 2, \ldots, n \tag{14}$$

For nonlinear fitting, the Eq. (14) is a nonlinear equation for a j, and the solution is difficult. In practical applications, the nonlinear function is usually linearized, such as by finding the matching function equations on both sides. Logarithmically, and then linearly fit to find the value of each parameter.

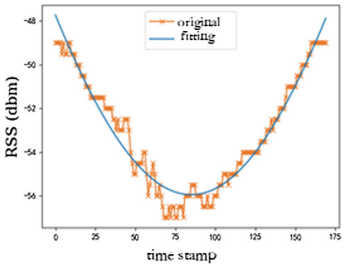

Fig. 5. Schematic diagram of curve fitting

Figure 5 is the fitted image of the "v" shaped area. According to theoretical analysis, the abscissa corresponds to the peak of the fitting curve (the valley of the "v" shaped region) is the time when the interference tag is closest to at the target tag. An in at the case the where at the direction of movement joining module of at the tag is known, knowing this moment, at the relative position of at the tag array can be determined by comparing at the order in which at the RSS peaks of at the tags in at the tag array appear. The in addition, if the moving speed of the interfering period tag is constant, the approximate distance between the two tags in the array can be obtained by multiplying the-difference between the peak times of the two tags by the moving speed of the tag.

Based on the above process, the data processing process of this model can be drawn, as shown in Fig. 6. Acquisition of the target tag to the RSS after values, first

average smoothing to remove jitter the data, eliminated the causal factors of space RSS interference value; secondly divided into areas, to find areas of interference, to filter out non- interference of related data; then through the DTW algorithm, the influence of the uneven sliding speed on the RSS timing is removed, so that the target sequence is as close as possible to the theoretical trend. Finally, the curve fitting is performed to find the minimum value of the RSS sequence, and the position of the corresponding interference tag is considered to be the location of the target tag.

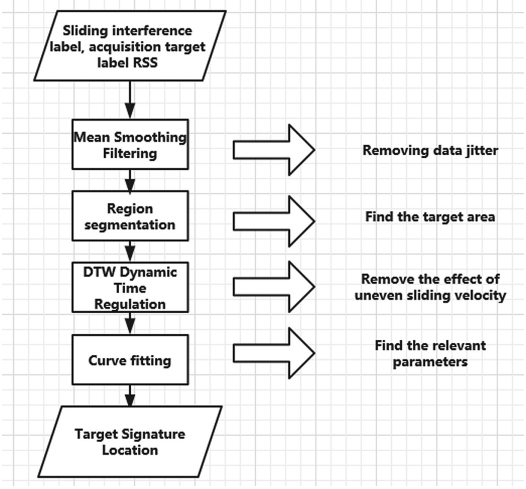

Fig. 6. Data processing process flow chart

6 Experiment and Evaluation

6.1 Experimental Environment

Figure 7 shows the main hardware devices used in the system, including RFID readers, reader antennas, RFID tags, and so on. The speedway r420 commercial UHF RFID reader manufactured by Impinj is used here. The reader complies with the EPC the global parameters.

R420 reader is connected. 4th laird a9028 type directional antenna, a gain of 8dbi, transmitting circularly polarized waves, in order to more effectively read the tag of different states, the main parameters of the antenna as illustrated.

This article uses the doc (alien 9741) type document tag produced by alien company of the united states. The tag has good anti-interference ability and can be placed at a close distance of multiple tags, which can effectively reduce the mutual occlusion between different tags, cardboard and similar printed matter dielectrics can be placed in many documents that are tightly wrapped by the tag without being missed by the reader [19]. The in addition, to the test performance of the model, uses this chapter the other six tags also, as shown in Fig. 8.

Fig. 7. System main hardware

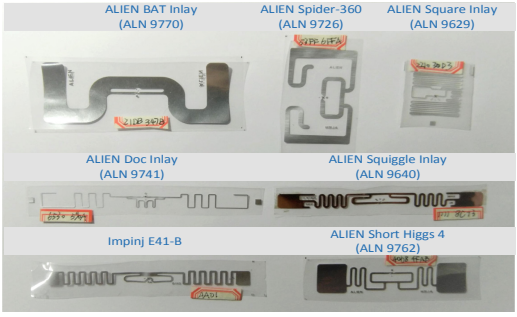

Fig. 8. Main tag used in this article

The system follows the EPC Global C1G2 protocol, and the operating frequency is 920.375–924.375 MHz in mainland China, with a total of 16 channels. R420 reader is connected to an Ethernet cable is equipped with 8 GB DDR4 memory, 256 GB PCIe SSD hard disk, the CPU is a 2.7 GHz clocked Intel Core i5-6200 the PC on board.

6.2 Robot Indoor Positioning Model Evaluation

Antenna Rotation Radian. To test the effect of the antenna's radius of rotation on the accuracy of the model, we deployed two antennas of the same model at two locations separated by 3.5 m. It gradually increases the radius of rotation of the antenna, the using the method of the third chapter of the estimated position of the tag, and the tag is determined to estimate the actual coordinates and the coordinate distance-difference, i.e., the positioning accuracy of the method. Other parameters during the experiment, such as the antenna's transmit power (32.5 dBm), transmission frequency (924.375 MHz), and tag ("doc" type), remain constant. The experimental results are shown in Fig. 9. Obviously, the accuracy of the system is stable within 20 cm when the radius of rotation is in the range of 12 to 17 cm. When the rotation is reduced

(<12 cm), the accuracy is getting worse. As stated in Sect. 3.3.2, this is due to the fact that the radius of rotation is too small and the distance difference caused by the rotation is not so obvious that the phase change is not obvious. When the radius of rotation is greater than 17 cm, since the maximum distance difference is greater than half a wavelength during rotation, a plurality of minimum values may be brought, resulting in an azimuth angle uncertainty, which is likely to cause a large error.

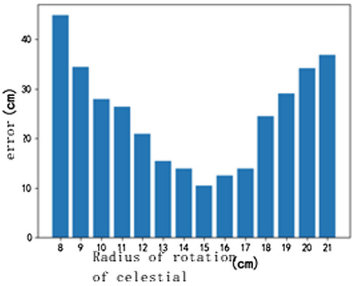

Fig. 9. Relationship between positioning error and antenna rotation radius

Antenna Rotation Radius. Of the two antennas spacing is another important factor affecting the accuracy of positioning (navigation). Here, the distance between the two antennas is gradually increased, and the coordinates of the tag are estimated at each distance. During the process, other factors remain the same, using the same tag all the time, and the antenna has a radius of rotation of 15 cm at each pitch. The results are shown in Fig. 10. It can be seen that from the overall trend the error increases with the increase of the spacing. In some cases, there is a case where the pitch is increased and the error is rather reduced. This is because when the antenna pitch is too close, the electromagnetic wave is reflected, interfered, or even diffracted by the opposite antenna, causing multipath, and the phase measurement value is largely deviated. In addition, the spacing of the antenna should not be too far, otherwise due to the characteristics of the AoA method, the deviation of the angle will become more and more obviously due to the increasing distance of the tag antenna, resulting in a large positioning error, based on the test results of this paper, the spacing of the antenna should be set at about 2.5 m.

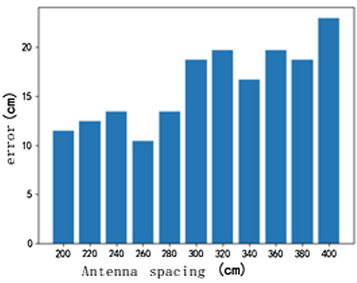

Fig. 10. Relationship between positioning error and antenna deployment spacing

The Impact of Tag-to-Antenna Distance. Here is another set of experiments: set the distance between the two antennas to 2.5 m, the radius of rotation of the antenna to 15 cm, move the tag on the mid-perpendicular line of the midpoint of the two antennas, and gradually increase the tag and the two antennas. The distance between the midpoint of the line (that is, the "foot" of the vertical line), the other parameters remain unchanged during the process, use this method to estimate the position coordinates of the tag, and the error between it and the calculate actual the position, the as shown in Fig. 11 shown. Of the farther is from the midpoint the tag of is two the antenna connections, the further from the is two the tag antennas. Obviously, in this process, the error continues to increase. The when the distance between the tag and the foot is 0.4 m, the distance between the tag and the two days is about 4.2 m, and the measurement error of the tag is as high 68 cm. It is foreseeable that as the distance increases, the error will continue to increase, which is clearly unacceptable.

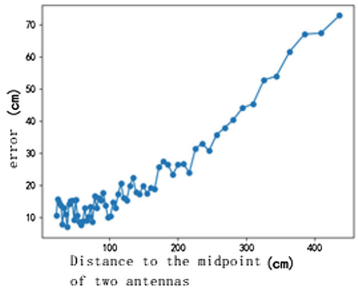

Fig. 11. Relationship between positioning error and tag antenna spacing

6.3 Evaluation of Robot Arm Grabbing Algorithm

The Impact of the Distance Between Two Interference Tags. To further determine the interference from the tag suitable place, here the following experiment: increasing the distance between the two interfering tag sequence *d* from 1 to 10 cm (i.e., u arms of the plate-shaped), in each under the spacing, the u-shaped plate with two interference tags is slid across the target tag, and the maximum drop amplitude of the target tag RSS at different intervals is recorded, and the experiment is repeated. Antenna the tags target and the keep stationary during the this other the process parameters and leave unchanged. Of the experimental results are shown in Fig. 12. when the distance between two the interference distance tags is 5 cm, the RSS of the target tag decreases the most, reaching 13 dBm. At other intervals, interference still exists, but it does not achieve optimal results.

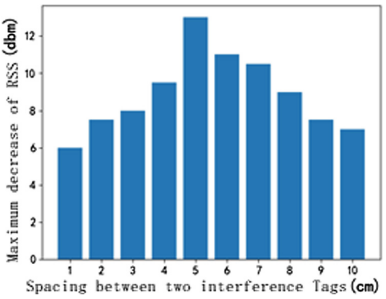

Fig. 12. Maximum drop in the target tag RSS when the tag is interspersed at different intervals

The Impact of Angle. As can be seen from the Fig. 13, the angle between the interference tag and the target tag affects the magnitude of the RSS drop. While the other conditions remain unchanged, the angle between the interference tag and the target tag is changed, and the interference tag is traversed by the target tag according to the fine-grained positioning model, and the position of the target tag is measured. Figure 13 shows the distance difference (error) between the coordinates of the position estimate and the actual coordinates at different angles. Obviously, the error increases with the increase of the angle, and the error between the two reaches the maximum when the angle is 90°. When the angle between the two is less than 45°, the mean value of the error is 1.9 cm, which indicates that the model can obtain higher accuracy. The actual deployment, this feature should be considered as much as possible, so that the interference tag and the target tag are as parallel as possible.

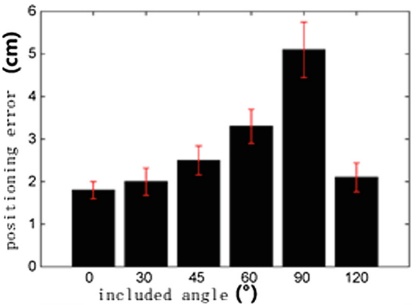

Fig. 13. Relationship between localization accuracy and the angle between two tags

Comparison with Existing Works. Figure 14 shows the use of stpp [13], rf-compass [20], tagoram [11], mobitagbot [14] and other existing work to locate the target tag when the average error. Wherein the rf-compass dependent on the stage in the signal processing software defined radio equipment (the usrp), expensive; and the stpp, tagoram, mobitagbot rely on commercial the rfid. Device the stpp is mainly used to obtain the sequence of the tag array, the average positioning accuracy. 8 cm & lt & lt around; tagoram the using multiple antennas, the hologram the using differential

algorithm can track a moving target, and obtain a higher accuracy (3.8 cm & lt); mobitagbot in the multipath effect has strong robustness in the strong scene, and the average error is about 2.8 cm. Compared with the above work, the proposed model algorithm can achieve an accuracy of 1.9 cm & lt. Compared to the require high computational complexity tagoram and required in the system in the initial stage of each of signal characteristics the measured on may be as a reference position mobitagbot, used in the this study location algorithm is lightweight, easy operation and high efficiency.

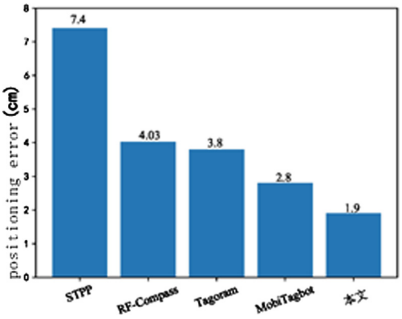

Fig. 14. Comparison between positioning accuracy and existing work

7 Conclusions

Robots have been increasingly applied to various real-world applications. This paper attempts to use RFID tags, which are widely deployed in warehousing and logistics, to help robots to navigate automatically and then locate targets. The paper is divided into two parts: rapid navigation of the robot and precise localization of the target. Extensive experimental results prove the effectiveness of proposed methods.

References

1. Finkenzeller, K., Wang, J., et al.: RFID Technology Principle and Application. Electronic Industry Press, Beijing (2015)
2. Knepper, R.A., Layton, T., Romanishin, J., et al.: IkeaBot: an autonomous multi-robot coordinated furniture assembly system. In: IEEE International Conference on Robotics and Automation, pp. 855–862. IEEE (2013)
3. Khoshelham, K., Elberink, S.O.: Accuracy and resolution of kinect depth data for indoor mapping applications. Sensors **12**(2), 1437 (2012)
4. Nirjon, S., Stankovic, J.A.: Kinsight: localizing and tracking household objects using depth-camera sensors. In: IEEE International Conference on Distributed Computing in Sensor Systems, pp. 67–74. IEEE (2012)
5. Biswas, J., Veloso, M.: WiFi localization and navigation for autonomous indoor mobile robots. In: International Conference on Robotics and Automation, pp. 4379–4384 (2010)

6. Ocana, M., Bergasa, L.M., Sotelo, M.A., et al.: Indoor robot navigation using a POMDP based on WiFi and ultrasound observations. In: IEEE/RSJ International Conference on Intelligent Robots and Systems, pp. 2592–2597. IEEE (2005)
7. Kothari, N., Kannan, B., Glasgwow, E.D., et al.: Robust indoor localization on a commercial smart phone. Proc. Comput. Sci. **10**(4), 1114–1120 (2012)
8. Wang, J., Katabi, D.: Dude, where's my card?: RFID positioning that works with multipath and non-line of sight. In: ACM SIGCOMM 2013 Conference on SIGCOMM, pp. 51–62. ACM (2013)
9. Yang, L., Chen, Y., Li, X.Y., et al.: Tagoram: real-time tracking of mobile RFID tags to high precision using COTS devices. In: International Conference on Mobile Computing and Networking, pp. 237–248. ACM (2014)
10. Wang, J., Vasisht, D., Katabi, D.: RF-IDraw: virtual touch screen in the air using RF signals. ACM SIGCOMM Comput. Commun. Rev. **44**(4), 235–246 (2014)
11. Shangguan, L., Yang, Z., Liu, A.X., et al.: Relative localization of RFID tags using spatial-temporal phase profiling. In: USENIX Conference on Networked Systems Design and Implementation, pp. 251–263. USENIX Association (2015)
12. Shangguan, L., Jamieson, K.: The design and implementation of a mobile RFID tag sorting robot. In: Proceedings of the 14th Annual International Conference on Mobile Systems, Applications, and Services, pp. 31–42. ACM (2016)
13. Ni, L.M., Liu, Y., Lau, Y.C., et al.: LANDMARC: indoor location sensing using active RFID. In: IEEE International Conference on Pervasive Computing and Communications, pp. 407–415. IEEE (2003)
14. Zhao, Y., Liu, Y., Ni, L.M.: VIRE: virtual reference elimination for active RFID-based localization. In: International Conference on Parallel Processing, p. 56. IEEE Xplore (2013)
15. Tse, D., Viswanath, P.: Fundamentals of Wireless Communication. Cambridge University Press, Cambridge (2005)
16. Yang, L., Lin, Q., Li, X., et al.: See through walls with cots RFID system! In: Proceedings of the 21st Annual International Conference on Mobile Computing and Networking, pp. 487–499. ACM (2015)
17. Duan, C., Yang, L., Liu, Y.: Accurate spatial calibration of RFID antennas via spinning tags. In: 2016 IEEE 36th International Conference on Distributed Computing Systems (ICDCS), pp. 519–528. IEEE (2016)
18. Han, J., Qian, C., Wang, X., et al.: Twins: device-free object tracking using passive tags. In: Proceedings of the IEEE INFOCOM 2014. IEEE (2014)
19. http://www.alientechnology.com/products/tags/doc/
20. Wang, J., Adib, F., Knepper, R., et al.: RF-compass: robot object manipulation using RFIDs. In: International Conference on Mobile Computing & Networking, pp. 3–14 (2013)